Spectroscopic Identification of Higher-Order Rare Gas−Dihalogen Complexes with Different Geometries: $He_{2,3}\cdots Br_2$ and $He_{2,3}\cdots ICl$

David S. Boucher,[†] Joshua P. Darr,[‡] David B. Strasfeld,[§] and Richard A. Loomis*

Department of Chemistry, Washington University in St. Louis, One Brookings Drive, CB 1134, Saint Louis, Missouri 63130

Received: September 20, 2008; Revised Manuscript Received: October 21, 2008

Rovibronic transitions of multiple conformers of the $He_2\cdots{}^{79}Br_2(X, v'' = 0)$, $He_3\cdots{}^{79}Br_2(X, v'' = 0)$, $He_2\cdots I^{35}Cl(X, v'' = 0)$, and $He_3\cdots I^{35}Cl(X, v'' = 0)$ complexes stabilized in a pulsed, supersonic expansion are observed in action spectra recorded in the B−X region of the dihalogens. In addition to features associated with $He_2\cdots{}^{79}Br_2$ and $He_2\cdots I^{35}Cl$ complexes with the rare gas atoms localized in the toroidal potential well lying in a plane perpendicular to the dihalogen bond, those associated with a ground-state conformer that has one He atom localized in the toroidal potential and the other He atom localized in the linear well at the end of the dihalogen moiety are also identified. Transitions of at least three conformers of the $He_3\cdots Br_2$ complex and two conformers of the $He_3\cdots ICl$ complex are also observed. The relative populations of the different conformers are found to depend on where along the supersonic expansion the spectra are recorded, and thus on the local temperature regime sampled. The $He_2\cdots{}^{79}Br_2$ and $He_2\cdots I^{35}Cl$ conformers with one He atom in each well are found to be the more stable conformers.

I. Introduction

The ability to stabilize van der Waals complexes and clusters in supersonic expansions has offered a convenient venue for studying long-range intermolecular forces and energy transfer mechanisms. Considerable attention has focused on the triatomic complexes, Rg···XY, consisting of a rare gas atom, Rg, weakly bound to a dihalogen chromophore, XY. Despite their structural simplicity, however, it is only recently that the details of the full multidimensional intermolecular potential energy surfaces (PESs) have become accurately characterized.[1−13] In related efforts, ties with bulk intermolecular energy transfer and solvation effects have been undertaken by investigating rare gas dihalogen clusters containing multiple rare gas atoms, $Rg_m\cdots XY$ ($m > 1$). Although extensive experimental and theoretical investigations have been reported on such systems, information concerning the multidimensionality of the PESs is still limited.

Previous experimental studies of $Rg_m\cdots XY$ clusters, such as $He_m\cdots I_2$ ($m = 2, 3$),[14] $Ne_m\cdots I_2$ ($m = 2-6$),[15] $He_lAr_m\cdots I_2$ ($l, m \geq 1$),[16] $Ne_m\cdots Br_2$ ($m = 2, 3$),[17] $Ne_m\cdots Cl_2$ ($m = 2, 3$),[18] and $Ne_m\cdots ICl$ ($m = 1-5$),[19] have revealed equilibrium structures in which all of the Rg atoms occupy equivalent positions around the dihalogen molecule. The toroidal potential energy well in which these Rg atoms are localized is axially symmetric about, and orthogonal to, the dihalogen bond and is commonly referred to as the T-shaped well. This structural information was deduced from rotationally resolved excitation spectra of the clusters recorded in the $B\ {}^3\Pi_{0+}-X\ {}^1\Sigma^+$ region of the dihalogen and simulations of the spectral features using asymmetric rigid-rotor models. In contrast to these clusters, structures could not be elucidated for the higher-order $He_m\cdots Cl_2$ complexes because of the somewhat coupled He−He motions about the Cl_2 molecule.[20−26]

Useful guidelines for identifying spectral features associated with transitions of the different $Rg_m\cdots XY$ complexes having a specific size, m, were established in these earlier investigations.[14] First, the positions of the higher-order features tend to follow a band-shift rule. This rule predicts that the vibronic transition energy of a $Rg_m\cdots XY$ complex is given by $\nu = \nu_0 + m\Delta\nu$, where ν_0 is the band origin of the XY monomer in the B−X, $v'-v''$ vibronic region and $\Delta\nu$ is a constant energy shift that represents the difference in the binding energies of the ground- and excited-state levels associated with the observed transition. Second, there is a strong propensity for weakly bound $Rg_m\cdots XY(B, v')$ complexes to dissociate into mRg + XY(B, $v'-m$) products.[26] One quantum of XY vibrational excitation dissociates each Rg atom because the excited-state binding energy of the complex is less than the XY vibrational level spacing. Also, the highest product channel for dissociating each Rg atom is the next lower XY vibrational level. An exception to this trend has been observed for $Ar_m\cdots I_2$ complexes, where the large binding energy associated with the excited-state complex, $\approx$234 cm^{-1}, dictates that three quanta of $I_2(B)$ vibrational excitation are typically necessary to dissociate each Ar atom.[27,28]

The Lester group showed that two-laser, action spectroscopy could be used to preferentially record spectra of complexes with a specific size.[29,30] In these experiments, a pump laser is scanned through a B−X, $v'-0$ vibronic region. A second probe laser is delayed in time from the pump laser and is fixed on an E−B, $v'-(v'-m)$ monomer transition. The signal associated with the probe laser is then monitored as a function of pump laser frequency to identify those transitions associated with $He_m\cdots XY$ complexes in the B−X, $v'-0$ region. For clarity, consider the scheme for pumping and probing $He_m\cdots{}^{79}Br_2$ complexes shown here:

* To whom correspondence should be addressed. E-mail: loomis@wustl.edu.

† Present address: Department of Chemistry & Biochemistry, Middlebury College, Middlebury, Vermont 05753.

‡ Present address: JILA, University of Colorado, Campus Box 440, Boulder, Colorado 80309.

§ Present address: Department of Chemistry, University of Wisconsin−Madison, Madison, Wisconsin 53706.

10.1021/jp808368j CCC: $40.75
Published on Web 12/03/2008

$$He_m\cdots{}^{79}Br_2(X, v''=0) + h\nu_{pump} \rightarrow He_m\cdots{}^{79}Br_2(B, v')$$

$$He_m\cdots{}^{79}Br_2(B, v') \rightarrow m\text{He} + {}^{79}Br_2(B, v) \quad \text{with} \quad v < v'$$

$${}^{79}Br_2(B, v) + h\nu_{probe} \rightarrow {}^{79}Br_2(E, v^{\dagger})$$

$${}^{79}Br_2(E, v^{\dagger}) \rightarrow {}^{79}Br_2(X, v'') + h\nu_{fluor}$$

Our group has utilized both laser-induced fluorescence (LIF) and two-laser, action spectroscopy techniques to provide evidence for the stabilization of ground-state complexes with linear geometries in addition to those with T-shaped, or near-T-shaped, geometries for both rare gas homonuclear and heteronuclear dihalogen complexes, He···ICl,[1,31,32] Ne···ICl,[33] He···Br_2,[3] He···I_2,[5] and Ar···I_2.[4] For each of these systems, discrete features associated with transitions of the linear complex to delocalized intermolecular vibrational levels are observed to energies greater than the monomer and T-shaped features. Furthermore, it was shown that it is possible to alter the expansion conditions and the region within the expansion being interrogated to vary the relative populations of the two conformers. For most of these systems, the linear conformer was found to be more strongly bound than the T-shaped conformer; the sole exception is the He···I_2(X, $v'' = 0$) complex, for which the T-shaped conformer was found to be slightly more stable than the linear conformer.[5]

The work presented in this manuscript extends this Rg···XY work to higher-order systems, Rg_m···XY, with $m > 1$, characterizing the spectroscopic signatures of the different conformers and demonstrating the ability to vary their relative populations. Specifically, we focus on the He_m···Br_2(X, $v'' = 0$) and He_m···ICl(X, $v'' = 0$) complexes to investigate the interactions of multiple helium atoms with a heteronuclear and a homonuclear dihalogen. We use two-laser, action spectroscopy as described above to identify the features associated with complexes containing different numbers of He atoms. We implement the band-shift rule to identify the ground-state conformers associated with each feature. The ability to interrogate clusters of varying size and with preferred geometries should broaden the study of vibrational predissociation dynamics in these systems and of multibody interactions and energy transfer mechanisms in general.

Throughout this manuscript we refer to conformers of the He_m···Br_2(X, $v'' = 0$) and He_m···ICl(X, $v'' = 0$) complexes having different geometries dictated by the minima about the dihalogen in which the He atoms are localized. The possibility of large-amplitude motions associated with the He atoms, as observed in He_m···Cl_2 clusters, precludes the use of point-group designations or geometrical descriptions based on rigid or average geometries. Therefore, in an effort to clarify the identities of the conformers, we use the notation (#T, #L)He_m···XY to denote their structures, where m = #T + #L. The number of He atoms localized in the toroidal potential about the dihalogen bond, typically referred to as the T-shaped well, is #T. The number of He atoms localized in the linear well at the end of the dihalogen molecule is #L; the linear well for He_m···ICl(X, $v'' = 0$) is at the iodine-atom end of the dihalogen. As an example, a He_3···Br_2(X, $v'' = 0$) ground-state complex with two He atoms localized in the toroidal potential and one He atom in the linear well will be referred to as the (2, 1)He_3···Br_2 conformer.

II. Experimental

Ground-state He_m···$^{79}Br_2$(X, $v'' = 0$) complexes with $m \geq 1$ were stabilized in a pulsed supersonic expansion generated by passing a He carrier gas through a sample cell containing liquid bromine and passing the He/Br_2 mixture through a 1 mm diameter pulsed-valve nozzle into a chamber maintained at a pressure <25 mTorr during operation. The Br_2 sample cell was maintained at a temperature of −15 °C so that a bromine vapor pressure of ≈0.03 bar was achieved. The helium backing pressure, P_0, was fixed at either 28.6 or 35.5 bar. Ground-state He_m···ICl(X, $v'' = 0$) complexes were generated by passing a pure He carrier gas through a vessel containing solid ICl held at 1 °C and pulsing the He/ICl mixture through an 800 μm nozzle into a vacuum chamber held at <25 mTorr during operation. The He carrier gas was typically maintained at P_0 = 14.8 bar relative to vacuum, which resulted an ICl concentration of ≈360 ppm under these conditions. A higher backing pressure of 28.6 bar was used to stabilize He_m···ICl(X, $v'' = 0$) complexes with up to $m = 4$.

Rovibronic spectra of the complexes were collected using LIF and two-laser, action spectroscopy.[29,30] The LIF spectra of the He_m···$^{79}Br_2$ and He_m···ICl complexes were recorded in the Br_2 B−X, 12−0 and ICl B−X, 3−0 regions using a Nd:YAG-pumped dye laser with a frequency resolution of 0.06 cm^{-1}. Typical pulse energies of <15 mJ were measured within the chamber after being spatially filtered to a diameter of 2−3 mm. The resultant B → X fluorescence was collected with a mirror and telescope assembly and imaged onto a photomultiplier tube (PMT). A 16.5 × 2.8 mm mask was positioned within the assembly with the long axis oriented parallel to the expansion direction so that only fluorescence from the centermost region of the expansion was collected. In order to block laser scatter and to collect the desired B → X fluorescence, 600 nm long-pass filters were positioned in front of the PMT. The signal was amplified and integrated with a gated boxcar integrator to record the fluorescence intensity as a function of the excitation laser energy.

Action spectra were obtained by scanning an excitation laser through a Br_2 or ICl B−X, v'−0 region and recording the fluorescence induced by a second probe laser, which is delayed by ≈20 ns in time from the first and is fixed on either a Br_2 or ICl E−B, $v^{\dagger}$−v transition. The excitation or pump laser was a 532 nm pumped dye laser operating in the Br_2 B−X, v'−0, with $v' = 12$, 13, or 14, or ICl B−X, 3−0 spectral regions with a frequency resolution of 0.06 cm^{-1}. The pulse energies were kept low enough, <5 mJ, to minimize saturation of the observed transitions but yet maintain satisfactory signal-to-noise levels in the spectra. For the He_m···$^{79}Br_2$ action spectra, the probe laser was the frequency-doubled output of a 532 nm pumped dye laser, and pulse energies were kept below 50 μJ. For the He_m···$I^{35}Cl$ action spectra, the probe laser was the output of a 355 nm pumped dye laser with pulse energies typically from 70 to 80 μJ. For both experiments, the spectral bandwidth of the probe laser was measured to be ≈0.06 cm^{-1}. A dichroic mirror was used to overlap and copropagate the pump and probe laser beams. The gently focused laser beams intersected the supersonic expansion at a specific reduced-downstream distance, $Z = x/d$, with x being the downstream distance and d the diameter of the pulsed-valve nozzle.

The resultant ion-pair-state fluorescence was collected with the same mirror/telescope and mask assembly described above and imaged onto a PMT with a high quantum efficiency in the ultraviolet region. Since dihalogen molecules and complexes promoted to levels within the E ion-pair state may experience nonadiabatic interactions and couple with the β and D′ states,[19,34−39] the fluorescence induced by the probe laser may be from any of these ion-pair states. A 15 nm band-pass filter

with a center wavelength of 267 nm was placed in front of the PMT to block laser scatter and to predominantly transmit Br_2 E → X fluorescence. A UG-1 filter was used to preferentially collect emission in the ICl E → X and to a lesser extent the ICl β → A and D′ → A′ spectral regions. The PMT signals were amplified and integrated with a gated boxcar integrator.

III. Results and Discussion

A. Spectroscopic Observation of Different $He_2\cdots{}^{79}Br_2$ and $He_3\cdots{}^{79}Br_2$ Conformers. The LIF spectrum recorded in the Br_2 B−X, 12−0 spectral region is plotted in Figure 1a as a function of energy from the $^{79}Br_2$ B−X, 12−0 band origin. The spectrum was acquired with $P_0 = 28.6$ bar and at $Z = 13$. The rotational temperature was determined to be 1.25(2) K by fitting the rotational contour of the $^{79}Br_2$ B−X, 12−0 band. The LIF spectrum is dominated by the intense T-shaped (1, 0)$He\cdots{}^{79}Br_2$ feature at 4 cm^{-1}, but features corresponding to transitions of the linear (0, 1)$He\cdots{}^{79}Br_2$(X, $v'' = 0$) conformer, centered near 10 cm^{-1}, and of the (2, 0)$He_2\cdots{}^{79}Br_2$(X, $v'' = 0$) higher-order complex, at 8 cm^{-1}, are also observed. The LIF spectra recorded in the Br_2 B−X, 13−0 and 14−0 regions have nearly the same intensity profiles and spectral shifts as shown in Figure 1a. The T-shaped and linear $He\cdots{}^{79}Br_2$ features have been characterized by us previously.[3] The assignment of the (2, 0)$He_2\cdots{}^{79}Br_2$ feature is based on the band-shift rule,[14] where we assume weak interactions between the two helium atoms. Since the T-shaped feature is observed at a transition energy of $\Delta\nu = +4$ cm^{-1} relative to the $^{79}Br_2$ B−X, 12−0 band origin, the band-shift rule predicts that the transition energy of the (2, 0)$He_2\cdots{}^{79}Br_2$ complex would be at $\nu = \nu_0 + m\Delta\nu = \nu_0 + 2(4)$ or $+8$ cm^{-1} relative to the monomer band origin, ν_0. Thus, the observed (2, 0)$He_2\cdots{}^{79}Br_2$ feature is precisely at the energy predicted by the band-shift rule.

As stated above, the $He_m\cdots XY$ complexes exhibit a general propensity for vibrational dissociation into the $\Delta v = -m$ channel. Action spectra obtained by fixing the probe laser on the band head of the $^{79}Br_2$ E−B, 1−11 transition and scanning the pump laser through the Br_2 B−X, 12−0 region should therefore be dominated by transitions of the $He_1\cdots{}^{79}Br_2$(X, $v'' = 0$) conformers. A $\Delta v = -1$ action spectrum obtained with the same conditions as implemented for the LIF spectrum, Figure 1a, is plotted in Figure 1b. The spectrum is plotted as a function of transition energy from the $^{79}Br_2$ B−X, 12−0 band origin. The action spectrum is nearly identical to the LIF spectrum, except the (2, 0)$He_2\cdots{}^{79}Br_2$ feature is not observed.

Additional action spectra were recorded to preferentially detect features associated with transitions of the $He_m\cdots{}^{79}Br_2$(X, $v'' = 0$) higher-order complexes. Action spectra that should identify $He_2\cdots{}^{79}Br_2$ and $He_3\cdots{}^{79}Br_2$ features in the Br_2 B−X, v'−0 region were acquired by fixing the probe laser on the $^{79}Br_2$ E−B, 1−11 transition and scanning the pump laser through the Br_2 B−X, 13−0 and 14−0 regions, respectively. The $He_m\cdots{}^{79}Br_2$ action spectra recorded while probing these $\Delta v = -2$ and -3 dissociation channels are shown in parts c and d, respectively, of Figure 1. The $\Delta v = -2$ spectrum was recorded with $P_0 = 28.6$ bar and the lasers intersecting the expansion at $Z = 16$. The $\Delta v = -3$ spectrum was recorded using a higher backing pressure, $P_0 = 35.5$ bar, and at a greater distance, $Z = 21$. Under these different expansion conditions, the rotational temperature of $^{79}Br_2$(X, $v'' = 0$) molecules was measured to be 0.93(3) K for the $\Delta v = -2$ action spectrum and 0.48(3) K for the $\Delta v = -3$ spectrum.

We assign the features in these action spectra as transitions of multiple conformers of different $He_m\cdots{}^{79}Br_2$(X, $v'' = 0$) complexes, including the (1, 0)$He_1\cdots{}^{79}Br_2$(X, $v'' = 0$) and (0, 1)$He_1\cdots{}^{79}Br_2$(X, $v'' = 0$) conformers at 4 and ≈10 cm^{-1}. The lifetimes of the $He_1\cdots{}^{79}Br_2$ complexes bound within the He + $^{79}Br_2$(B, $v' = 13$) and He + $^{79}Br_2$(B, $v' = 14$) potentials are short, <100 ps.[40,41] These $He_1\cdots{}^{79}Br_2$ features are observed in the $\Delta v = -2$ and -3 action spectra because of rapid $He_1\cdots{}^{79}Br_2$(B, $v' = 13, 14$) dissociation into the $\Delta v = -1$ channel, followed by the collisional relaxation of the resultant $^{79}Br_2$(B, $v' = 12, 13$) fragments down to the $^{79}Br_2$(B, $v' = 11$) molecular level. The high backing pressures used to stabilize

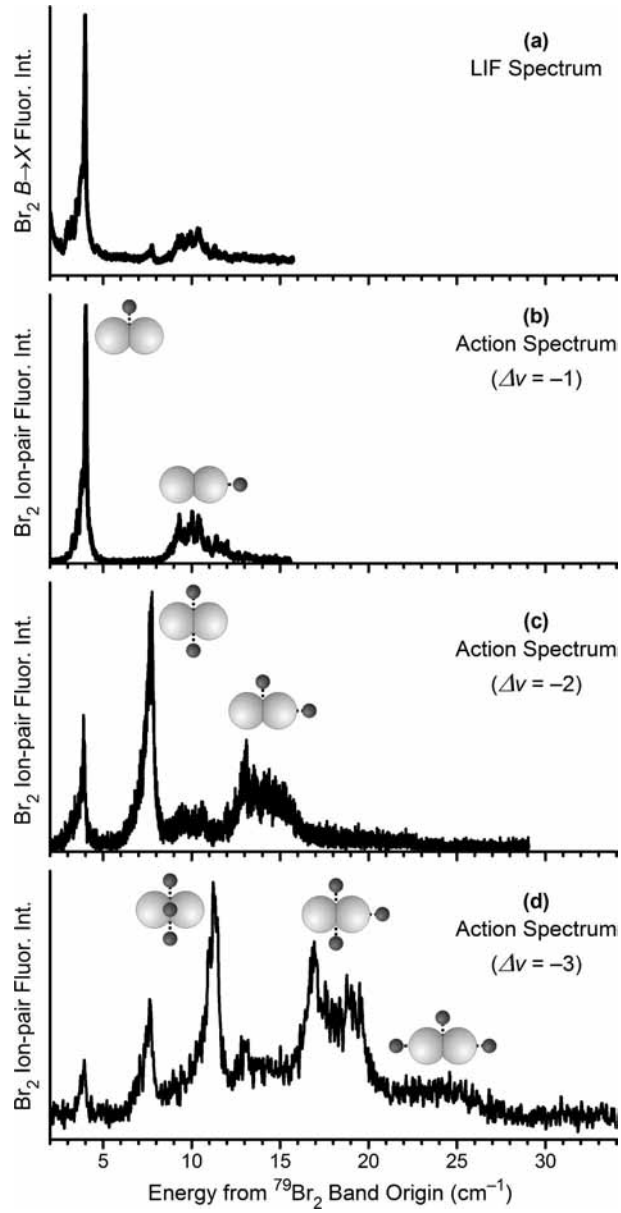

Figure 1. Laser-induced fluorescence, LIF (a), and action spectra, (b), (c), and (d), of $He_m\cdots Br_2$ complexes plotted as a function of energy from the corresponding $^{79}Br_2$ B−X, v'−0 band origin. The LIF spectrum was recorded in the 12−0 region, and the action spectra in (a), (b), and (c) were recorded by fixing the probe laser on the band head of the $^{79}Br_2$ E−B, 1−11 transition and scanning the excitation laser through the 12−0, 13−0, and 14−0 spectral regions in order to detect $^{79}Br_2$(B) products in the $\Delta v = -1$, -2, and -3 dissociation channels, respectively. The spectra in (a) and (b) were acquired using a backing pressure, P_0, of 28.6 bar and at a reduced-downstream distance of $Z = 13$. The same P_0 was used for (c), but at $Z = 16$. The spectrum in (d) was recorded with $P_0 = 35.5$ bar and at $Z = 21$. The cartoons indicate the geometries of the ground-state $He_m\cdots{}^{79}Br_2$(X, $v'' = 0$) conformer associated with each feature.

these higher-order complexes, 28.6 and 35.5 bar, and the ≈20 ns delay between the pump and probe lasers should be sufficient for this collisional relaxation. When using lower backing pressures, the intensities of the $He_1\cdots{}^{79}Br_2$ features decrease relative to those of the $He_m\cdots Br_2$ higher-order features, thereby confirming the role of collisions in observing the $He_1\cdots{}^{79}Br_2$ features.

The additional features in the $\Delta v = -2$ and -3 action spectra, parts c and d of Figure 1, are attributed to transitions of the $He_2\cdots{}^{79}Br_2(X, v'' = 0)$ and $He_3\cdots{}^{79}Br_2(X, v'' = 0)$ higher-order complexes based on their appearance in the different Δv action spectra, their relative intensities, and their energies relative to the corresponding band origin. For instance, features associated with transitions of the $He_3\cdots{}^{79}Br_2(X, v'' = 0)$ higher-order complexes are not expected to be in the action spectra obtained with the probe laser fixed on transitions of the $\Delta v = -2$ dissociation channel. Although features attributed to $He_2\cdots{}^{79}Br_2(X, v'' = 0)$ complexes may be observed in the $\Delta v = -3$ spectra, the intensity of the $He_3\cdots{}^{79}Br_2(X, v'' = 0)$ features should be significantly enhanced relative to the $He_2\cdots{}^{79}Br_2(X, v'' = 0)$ features because of collisional relaxation of the molecular products.

A slightly modified version of the band-shift rule was employed to support these assignments and to identify the particular ground-state geometry of the higher-order conformers associated with each feature. Specifically the energy of a feature associated with transitions of a (#T, #L)$He_m\cdots{}^{79}Br_2(X, v'' = 0)$ higher-order complex is expected to follow $\nu = \nu_0 + \{(\#T)\Delta\nu_T + (\#L)\Delta\nu_L\}$, where ν_0 is the monomer band origin and $\Delta\nu_T$ and $\Delta\nu_L$ are the energetic shifts of the T-shaped and linear features from the monomer band origin, respectively. For example, a feature associated with a transition of the (2, 0)$He_2\cdots{}^{79}Br_2(X, v'' = 0)$ conformer would be shifted from the monomer band origin by $\approx\{2(4) + 0(0)\}$ cm^{-1} = +8 cm^{-1}. In contrast, a feature associated with a transition of the (1, 1)$He_2\cdots{}^{79}Br_2(X, v'' = 0)$ conformer would be shifted by $\approx\{1(4) + 1(10)\}$ cm^{-1} = +14 cm^{-1} from the monomer band origin.

In addition to the small T-shaped and linear $He\cdots{}^{79}Br_2(X, v'' = 0)$ features, there are features attributable to transitions of five more complexes: two $He_2\cdots{}^{79}Br_2(X, v'' = 0)$ conformers and three $He_3\cdots{}^{79}Br_2(X, v'' = 0)$ conformers. The features at ≈8 and 14 cm^{-1}, which have significant intensity in the $\Delta v = -2$ action spectra, have been assigned to the (2, 0)$He_2\cdots{}^{79}Br_2$ and (1, 1)$He_2\cdots{}^{79}Br_2$, respectively. The dominant feature in the $\Delta v = -3$ spectrum, at ≈11.5 cm^{-1}, is ascribed to transitions of the (3, 0)$He_3\cdots{}^{79}Br_2(X, v'' = 0)$ conformer. This feature would be expected at $\approx\{3(4) + 0(10)\}$ cm^{-1} = +12 cm^{-1}, which is close to that observed in the spectrum. The intense and rather broad band in the $\Delta v = -3$ spectrum, spanning from 17 to 21 cm^{-1}, is attributed to the (2, 1)$He_3\cdots{}^{79}Br_2(X, v'' = 0)$ conformer. The predicted energy for this feature is $\approx\{2(4) + 1(10)\}$ cm^{-1} = +18 cm^{-1}. Lastly, the broad feature extending toward higher energies is attributed to transitions of the (1, 2)$He_3\cdots{}^{79}Br_2(X, v'' = 0)$ conformer, which is predicted to be at transition energies of $\approx\{1(4) + 2(10)\}$ cm^{-1} = +24 cm^{-1} from the band origin. We presume that this ground-state complex is the linear conformer with one He atom localized in each end of the Br_2 molecule, and one in the T-shaped well. We base this assignment on the calculations for the $He_2 + Br_2(X, v'' = 0)$ interactions that indicate that the linear (0, 2)$He_2\cdots Br_2$ is significantly more stable than a (0, 2)$He_2\cdots Br_2$ conformer with both He atoms in the same well at one end of the Br_2 molecule.[42]

The shapes of the rotational contours of the different features support these assignments. As mentioned above, previous studies of $Rg_m\cdots XY$ higher-order complexes for which structures could be elucidated revealed "belt" configurations with the rare gas atoms localized in the T-shaped well. The rotational contours of these features were nearly the same as those of the T-shaped $Rg\cdots XY$ triatomic complexes, such as that of the (1, 0)$He\cdots{}^{79}Br_2$ feature. The position of the He atom in the T-shaped well in both the ground and excited states barely changes the rotational constant away from that of the dihalogen molecule.[5] As a result, there is a distinct band head at low rotational lines of the R branch, and the feature extends toward lower transition energies with decreasing intensity. Similar rotational contours are observed for the (2, 0)$He_2\cdots{}^{79}Br_2$ and (3, 0)$He_3\cdots{}^{79}Br_2$ features. The rotational contour of the linear (1, 0)$He\cdots{}^{79}Br_2$ feature is distinctly different. Transitions from a ground-state level with a He atom localized at the linear end of the dihalogen to intermolecular vibrational levels with the He atom delocalized along the angular coordinate about the dihalogen molecule give rise to complicated rotational contours that are distinctly different from those of the dihalogens.[1,3,5] These contours exhibit significantly more rotational structure, and the most intense rotational lines tend to be toward the lower-energy region of the feature. Calculations indicate that transitions of the linear conformer to multiple intermolecular vibrational levels with small energy spacings within the excited state contribute to the spectral congestion within the linear features.[3] The rotational contours of the (1, 1)$He_2\cdots{}^{79}Br_2$, (2, 1)$He_3\cdots{}^{79}Br_2$, and (1, 2)$He_3\cdots{}^{79}Br_2$ features resemble that of the linear (0, 1)$He\cdots{}^{79}Br_2$ feature.

The action spectra acquired using different probe transitions indicate that multiple conformers of the $He\cdots{}^{79}Br_2(X, v'' = 0)$, $He_2\cdots{}^{79}Br_2(X, v'' = 0)$, and $He_3\cdots{}^{79}Br_2(X, v'' = 0)$ complexes can be stabilized in a supersonic expansion. These conformers have distinct rovibronic features at transition energies that follow a simple band-shift rule. The fact that the features associated with transitions of the $He_m\cdots{}^{79}Br_2(X, v'' = 0)$ higher-order complexes are not clearly discernible in the LIF spectra indicate their populations are significantly lower than that of the $He\cdots{}^{79}Br_2(X, v'' = 0)$ complexes when using the described conditions.

B. Spectroscopic Observation of Different $He_2\cdots I^{35}Cl$ and $He_3\cdots I^{35}Cl$ Conformers. The LIF spectra and $\Delta v = -1$ action spectra of ICl entrained in a He-carrier gas contain features in the ICl B−X, 3−0 region that are associated with transitions of the different conformers of the $He\cdots ICl(X, v'' = 0)$ complex.[2,32,43] The features associated with transitions of the T-shaped (1, 0)$He\cdots I^{35}Cl(X, v'' = 0)$ and linear (0, 1)$He\cdots I^{35}Cl(X, v'' = 0)$ conformers are observed at ≈3.5 and ≈14.5 cm^{-1}, respectively. The LIF spectrum in Figure 2a was collected at $Z = 11.9$, and fitting the $I^{35}Cl$ B−X, 2−0 rovibronic band contour yielded an $I^{35}Cl(X, v'' = 0)$ rotational temperature of 1.49(3) K for these conditions. The $\Delta v = -1$ action spectrum recorded by scanning the pump laser through the ICl B−X, 3−0 region with the probe laser fixed on the $I^{35}Cl$ E−B, 11−2 transition is shown in Figure 2b. The reduced-downstream distance was slightly shorter, $Z = 8.8$, and a warmer $I^{35}Cl(X, v'' = 0)$ rotational temperature of 2.34(3) K was measured. The prominent difference between the spectra in parts a and b of Figure 2 is the absence of the feature associated with transitions of the linear (0, 1)$He\cdots I^{37}Cl(X, v'' = 0)$ conformer at ≈7.5 cm^{-1} in the action spectrum.

The $\Delta v = -2$ action spectrum plotted in Figure 2c was recorded under the same conditions as Figure 2b, except that

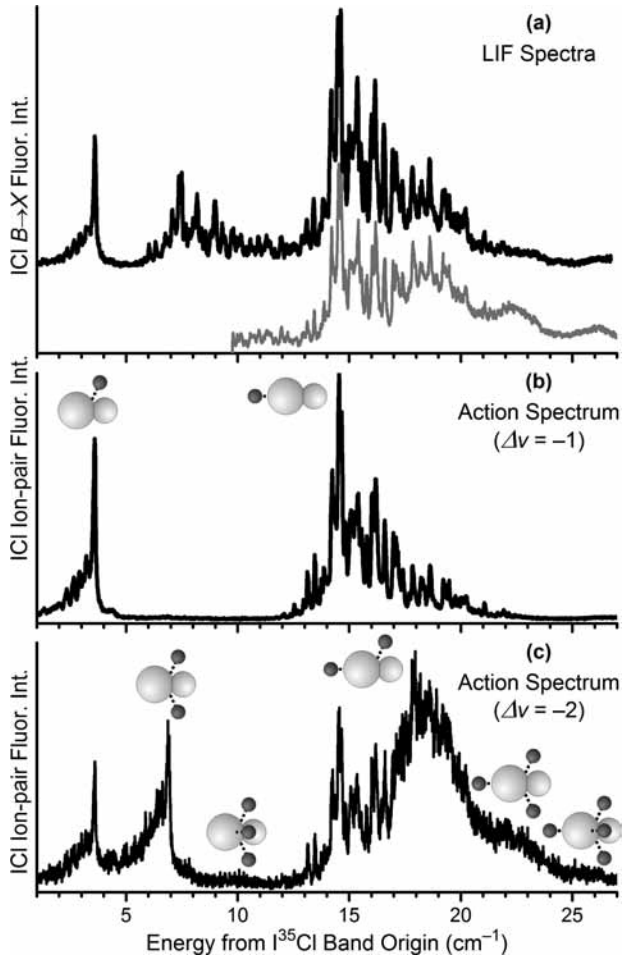

Figure 2. Laser-induced fluorescence, LIF (a) and action spectra (b) and (c) of $He_m\cdots ICl$ complexes recorded in the ICl B−X, 3−0 spectral region. The spectra are plotted as a function of energy from the $I^{35}Cl$ B−X, 3−0 band origin. The action spectra in (b) and (c) were acquired with the probe laser fixed on the band heads of the $I^{35}Cl$ E−B, 11−2 and $I^{35}Cl$ E−B, 9−1 transitions to probe the $I^{35}Cl(B)$ products in the $\Delta v = -1$ and −2 dissociation channels, respectively. The spectra were recorded using a He backing pressure of 14.8 bar with the exception of the gray LIF spectrum in (a), which utilized a pressure of 28.6 bar. The LIF spectra were obtained at reduced-downstream distance of $Z = 11.9$, while the action spectra were obtained at $Z = 8.8$. The cartoons indicate the geometries of the ground-state $He_m\cdots I^{35}Cl(X, v'' = 0)$ conformer associated with each feature. The broad feature in (a), with a maximum intensity near 7.5 cm^{-1}, is associated with a $He\cdots I^{37}Cl$ isotopomer.

the probe laser was fixed on the $I^{35}Cl$, E−B, 9−1 transition. The (1, 0) and (0, 1)$He\cdots I^{35}Cl$ features are still present in the spectrum, but they are no longer the most intense features. In comparison to the $\Delta v = -1$ action spectrum two additional features appear, one at ≈7 cm^{-1} and another at ≈18 cm^{-1} from the monomer band origin. The feature at ≈7 cm^{-1} is associated with transitions of the (2, 0)$He_2\cdots I^{35}Cl(X, v'' = 0)$ conformer based on the band-shift rule, $\nu = \nu_0 + \{(\#T)\Delta\nu_T + (\#L)\Delta\nu_L\} = \nu_0 + \{2(3.5) + 0(14.5)\}$ cm^{-1} or a shift of ≈+7 cm^{-1} from the $I^{35}Cl$ B−X, 3−0 band origin. The similarity of the rotational contour in comparison to the T-shaped (1, 0)$He\cdots I^{35}Cl$ feature further suggests that this feature is associated with transitions of the (2, 0)$He_2\cdots I^{35}Cl$ complex. In Figure 2c, the rotational contour of the feature at ≈18 cm^{-1} is similar to that of the linear (0, 1) feature with a maximum at 14.5 cm^{-1} in Figure 2b, but with even greater spectral congestion. The band-shift rule predicts a transition energy of ≈{1(3.5) + 1(14.5)} cm^{-1} = +18 cm^{-1}, relative to the monomer band origin, for the (1, 1)$He_2\cdots I^{35}Cl$ feature. Based on these shape and energy criteria, we assign the feature at ≈18 cm^{-1} to transitions of the (1, 1)$He_2\cdots I^{35}Cl(X, v'' = 0)$ conformer.

Interestingly, there is an extremely weak feature observed at ≈7 cm^{-1} in the $\Delta v = -1$ action spectrum, Figure 2b, the same transition energy as the (2, 0)$He_2\cdots I^{35}Cl$ feature in the $\Delta v = -2$ action spectrum. Closer inspection of this feature reveals that it has the same rotational contour as the (2, 0)$He_2\cdots I^{35}Cl$ feature. The presence of this feature in the $\Delta v = -1$ action spectrum suggests that a small fraction of the (2, 0)$He_2\cdots I^{35}Cl$ complexes promoted to the lowest-lying intermolecular vibrational level within the $2He + I^{35}Cl(B, v' = 3)$ PES dissociates into the $2He + I^{35}Cl(B, v' = 2)$ product channel. Additionally, there is a weak feature at ≈10 cm^{-1} in the $\Delta v = -2$ action spectrum plotted in Figure 2c. Using the band-shift rule, we would predict that the (3, 0)$He_3\cdots I^{35}Cl$ feature would be at a transition energy of ≈{3(3.5) + 0(14.5)} cm^{-1} = +10.5 cm^{-1}. We associate this feature with transitions of the (3, 0)$He_3\cdots I^{35}Cl(X, v'' = 0)$ conformer to the lowest intermolecular vibrational level lying within the $3He + I^{35}Cl(B, v' = 3)$ PES. Thus, a small fraction of the excited-state complexes in this lowest energy level apparently undergo dissociation into the $\Delta v = -2$ products.

Two additional weak, structureless features are observed at ≈22 and 26 cm^{-1} in the $\Delta v = -2$ action spectrum, Figure 2c. Using the band-shift rule, we would predict that a (2, 1)$He_3\cdots I^{35}Cl$ feature would be shifted by ≈{2(3.5) + 1(14.5)} cm^{-1} = +21.5 cm^{-1} from the monomer band origin. Additionally, a (3, 1)$He_4\cdots I^{35}Cl$ feature would be expected to be at a transition energy of ≈{3(3.5) + 1(14.5)} cm^{-1} = +25 cm^{-1}. While we did not anticipate observing (2, 1)$He_3\cdots I^{35}Cl$ or (3, 1)$He_4\cdots I^{35}Cl$ features in the $\Delta v = -2$ action spectra, we also did not expect to observe a (2, 0)$He_2\cdots I^{35}Cl$ feature in the $\Delta v = -1$ spectrum, Figure 2b, or a (3, 0)$He_3\cdots I^{35}Cl$ feature in the $\Delta v = -2$ spectrum, Figure 2c. Unfortunately, it is difficult to access distinct transitions in the ICl E−B, $v^{\dagger}$−0 region with the current experimental configuration, and we were not able to better characterize these features by recording $\Delta v = -3$ action spectra in the ICl B−X, 3−0 region. Additional LIF and action spectra were recorded using higher He backing pressures in order to increase the propensity for forming larger $He_m\cdots ICl(X, v'' = 0)$ complexes. The higher-energy region of an LIF spectrum recorded with a backing pressure of 28.6 bar is plotted in Figure 2a, gray spectrum. The relative intensities of the broadened features at 22 and 26 cm^{-1} increase significantly in comparison to the (0, 1) and (1, 1) features at ≈14.5 and ≈18 cm^{-1}, respectively, which both contain distinct rotational lines. This trend suggests that the complexes associated with these features are either larger-order complexes, with $m \geq 3$, or that they are energetically more stable conformers of the $He\cdots ICl$ or $He_2\cdots ICl$ complexes. The latter possibility can be ruled out because the band-shift rule does not predict $He\cdots ICl$ or $He_2\cdots ICl$ features at these energies. As a result, we attribute the features at ≈22 and 26 cm^{-1} to transitions of the (2, 1)$He_3\cdots I^{35}Cl(X, v'' = 0)$ and (3, 1)$He_4\cdots I^{35}Cl(X, v'' = 0)$ ground-state complexes.

These spectroscopic studies indicate that at least two conformers of the $He_2\cdots I^{35}Cl(X, v'' = 0)$ and $He_3\cdots I^{35}Cl(X, v'' = 0)$ complexes can be stabilized in a supersonic expansion, and these conformers have the (2, 0)$He_2\cdots I^{35}Cl$, (1, 1)$He_2\cdots I^{35}Cl$, (3, 0)$He_3\cdots I^{35}Cl$, and (2, 1)$He_3\cdots I^{35}Cl$ configurations. Unexpectedly, features associated with transitions of $He_2\cdots I^{35}Cl$ complexes were observed in $\Delta v = -1$ action spectra. Additionally, the $\Delta v = -2$ action spectrum contains

features associated with transitions of $He_3\cdots I^{35}Cl$ and $He_4\cdots I^{35}Cl$ complexes. Thus, these weakly bound complexes do not rigorously follow the trend for dissociation of $Rg_m\cdots XY(B, v')$ complexes into $mRg + XY(B, v'-m)$ products. These experiments do not provide insights into the dissociation mechanism for these unexpected dissociation pathways, but an intramolecular vibrational relaxation mechanism similar to that proposed for dissociation of $Ne\cdots Br_2(B,v')$ complexes seems probable.[44,45]

C. Determination of the Relative Stability of the $He_2\cdots{}^{79}Br_2$ and $He_2\cdots I^{35}Cl$ Conformers. Since different conformers of the $He_2\cdots{}^{79}Br_2(X, v'' = 0)$ and $He_2\cdots I^{35}Cl(X, v'' = 0)$ higher-order complexes have been spectroscopically identified, we have undertaken systematic studies to identify which conformers are energetically more stable. Specifically, we have recorded $\Delta v = -2$ action spectra at varying pressures and at increasing downstream distances to interrogate how the relative populations of these conformers change along the supersonic expansion. By using higher backing pressures, not only can complexes with additional He atoms be stabilized,[46] but the collisions can shift the relative populations of different conformers to those levels that are more strongly bound. In a similar manner, spectra recorded at longer downstream distances interrogate colder temperature regions, and the populations may shift toward the energetically preferred levels.

Action spectra of $He_2\cdots{}^{79}Br_2$ complexes were acquired in the Br_2 B−X, 13−0 region in the same manner as described above, but at $Z = 13.1$ and with two different backing pressures, $P_0 = 28.6$ and 35.5 bar. The peak intensity of the (2, 0)$He_2\cdots{}^{79}Br_2$ feature relative to that of the (1, 1)$He_2\cdots{}^{79}Br_2$ feature decreased from ≈2.3 down to ≈2.0 with the increase in backing pressure. The intensities of the (1, 0)$He\cdots{}^{79}Br_2$ and (0, 1)$He\cdots{}^{79}Br_2$ features both increased with the higher backing pressures, indicating the role of collisional relaxation in observing these features in the $\Delta v = -2$ action spectra. We chose not to do a more quantitative comparison of the integrated intensities of different $He_2\cdots{}^{79}Br_2$ bands, because of the spectral overlap of the (0, 1)$He\cdots{}^{79}Br_2$ feature with both the (2, 0)$He_2\cdots{}^{79}Br_2$ and (1, 1)$He_2\cdots{}^{79}Br_2$ features. Nevertheless, a distinct and reproducible increase in the relative intensity of the (1, 1)$He_2\cdots{}^{79}Br_2$ feature indicates that with the higher backing pressure, and thus additional collisions, the relative population of this conformer increases.

As stated above, the peak intensity of the (2, 0)$He_2\cdots{}^{79}Br_2$ feature was ≈2.3 times greater than the peak of the (1, 1)$He_2\cdots{}^{79}Br_2$ feature in the $\Delta v = -2$ action spectrum acquired with $P_0 = 28.6$ bar and at $Z = 13.1$. The $^{79}Br_2(X, v'' = 0)$ rotational temperature was measured to be 1.07(5) K when using these conditions. Using the same 28.6 bar helium backing pressure, but at a greater reduced-downstream distance, $Z = 18.7$, the rotational temperature decreased to 0.62(2) K. At this distance and rotational temperature, the peak intensity of the (2, 0)$He_2\cdots{}^{79}Br_2$ feature relative to the (1, 1)$He_2\cdots{}^{79}Br_2$ feature dropped to a factor of 1.8. This temperature dependence provides additional evidence that the (1, 1)$He_2\cdots{}^{79}Br_2(X, v'' = 0)$ conformer is more strongly bound than the (2, 0)$He_2\cdots{}^{79}Br_2(X, v'' = 0)$ conformer.

The subtle changes in the relative intensities of the $He_2\cdots{}^{79}Br_2$ features, and hence in the relative populations of the two conformers, indicate that the binding energies of the two conformers are nearly the same. This conclusion is consistent with the slight differences in the binding energies of the T-shaped (1, 0)$He\cdots{}^{79}Br_2(X, v'' = 0)$ and linear (0, 1)$He\cdots{}^{79}Br_2(X, v'' = 0)$ conformers; the binding energy of the linear conformer was measured to be 17.0(8) cm^{-1}, and that of the T-shaped conformer was estimated to be slightly less, 16.6(8) cm^{-1}.[3] Considering the effectiveness of the band-shift rule in predicting the energies of the higher-energy features, the interactions of the He atoms within the $He_2\cdots{}^{79}Br_2(X, v'' = 0)$ complexes must be negligible. We therefore conclude that the (1, 1)$He_2\cdots{}^{79}Br_2(X, v'' = 0)$ conformer is ≈0.4 cm^{-1} more stable than the (2, 0)$He_2\cdots{}^{79}Br_2(X, v'' = 0)$ conformer, as described in the next section.

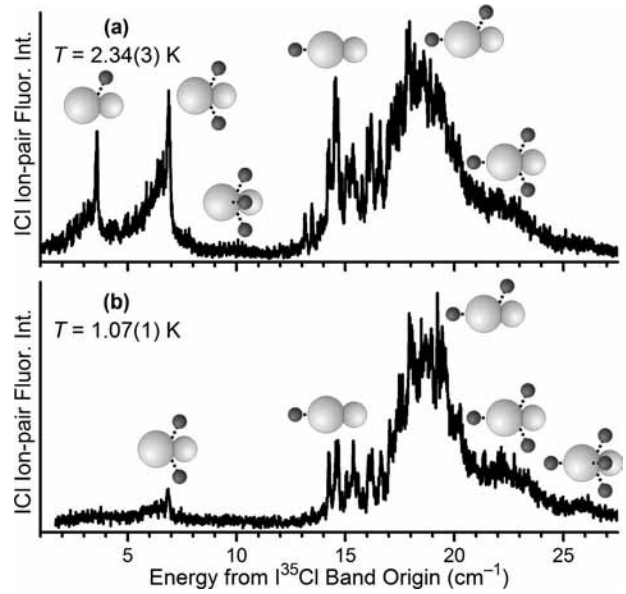

Figure 3. Action spectra recorded in the ICl B−X, 3−0 spectral region with the probe laser fixed on the band head of the $I^{35}Cl$ E−B, 9−1 transition. The spectra are plotted as a function of energy from the $I^{35}Cl$ B−X, 3−0 band origin. The spectra were recorded using a He backing pressure of 14.8 bar and at reduced-downstream distances of $Z = 8.8$ and 19.1 for (a) and (b), in order to probe different temperature regimes along the expansion. The $I^{35}Cl$ monomer rotational temperatures measured when using these conditions are listed. The cartoons indicate the geometries of the ground-state conformer associated with each feature.

The changes in the relative intensities of the (2, 0)$He_2\cdots I^{35}Cl$ and (1, 1)$He_2\cdots I^{35}Cl$ features observed in $\Delta v = -2$ action spectra with increasing backing pressure and downstream distance are more pronounced than those observed for $He_2\cdots{}^{79}Br_2$ with increasing backing pressure and downstream distance. At a given downstream distance, the peak intensity of the (1, 1)$He_2\cdots I^{35}Cl$ feature typically increased by a factor of 2−3 relative to that of the (2, 0)$He_2\cdots I^{35}Cl$ feature when increasing P_0 from 8.3 to 14.8 bar. The changes in the intensities of the features were even more dramatic with increasing distance along the expansion. As shown in Figure 3, the intensity of the (2, 0)$He_2\cdots I^{35}Cl$ feature in the $\Delta v = -2$ action spectrum decreases by a factor of 8 in moving from $Z = 8.8$ to 19.1 when using $P_0 = 14.8$ bar. At the same time, the intensity of the (1, 1)$He_2\cdots I^{35}Cl$ feature remains intense. The fits of the $I^{35}Cl$ B−X, 2−0 rotational contours measured at these distances indicate the rotational temperature decreases from 2.34(3) K down to 1.07(1) K for $Z = 8.8$ and $Z = 19.1$, respectively. These dependences indicate that the conformer with one He atom localized in the linear well, (1, 1)$He_2\cdots I^{35}Cl(X, v'' = 0)$, is energetically more stable than the (2, 0) conformer, which has both He atoms in the T-shaped well. The $\Delta v = -2$ action spectra also reveal the relative stabilities of the two observed conformers of the $He_3\cdots I^{35}Cl(X, v'' = 0)$ complexes. The intensity of the (3, 0)$He_3\cdots I^{35}Cl$ feature is weak but measurable

at a reduced-downstream distance of $Z = 8.8$. This same feature is not detected further downstream. The intensity of the (2, 1) feature, in contrast, increases slightly with cooling. This data suggest that the (2, 1)$He_3\cdots I^{35}Cl(X, v'' = 0)$ conformer is more strongly bound than the (3, 0)$He_3\cdots I^{35}Cl(X, v'' = 0)$ conformer.

Simulations of the stabilization of T-shaped and linear $Ar\cdots I_2(X, v'' = 0)$ complexes[47] offer insights into two mechanisms by which collisions with He atoms may facilitate the conversion of complexes between the different conformers even at very low temperatures. Although these simulations focused on the triatomic $Ar\cdots I_2$ complexes, the mechanisms should also apply to the conversion of higher-order complexes. The first mechanism is a conventional collision-induced isomerization reaction. The approaching He atom gains kinetic energy as a result of the attraction associated with the van der Waals potential between the atom and the complex. This kinetic energy results in an increase in the internal energy of the collision complex, perhaps above the barrier for motion of the originally bound He atom along the angular coordinate. The bound He atom can become restabilized in a different potential minimum with the colliding He atom taking away the excess energy. The second mechanism is an exchange reaction or swap mechanism. The colliding He atom approaches a well of the $He_m\cdots XY$ cluster, forming a metastable $He_{m+1}\cdots XY$ collision complex. The internal energy of the collision complex is raised, a He atom initially localized in a higher-energy minimum is ejected, and an energetically more stable $He_m\cdots XY$ conformer is formed. The dominant mechanism for conversion between different conformers of rare gas−dihalogen complexes is unknown, but either of these two mechanisms could be envisaged for the conversion of the (2, 0)$He_2\cdots{}^{79}Br_2(X, v'' = 0)$ and (2, 0)$He_2\cdots I^{35}Cl(X, v'' = 0)$ conformers to the more thermodynamically stable (1, 1) configurations.

There are no spectroscopic features that can be attributed to transitions of the (0, 2)$He_2\cdots{}^{79}Br_2(X, v'' = 0)$ conformer, which would be expected at an energy of 20 cm^{-1} using the band-shift rule. As will be discussed in the next section, this conformer has been calculated to be the most stable of the $He_2\cdots{}^{79}Br_2(X, v'' = 0)$ conformers.[42] We also do not observe spectroscopic features that can be associated with the antilinear (0, 1)$He\cdots I^{35}Cl(X, v'' = 0)$ conformer, which is predicted to be at significantly higher energy than the linear (0, 1) or T-shaped (1, 0) conformers.[2] In addition, all of the observed features follow the band-shift rule using the linear or T-shaped energies, and there are no other features that could be associated with a $He_m\cdots I^{35}Cl(X, v'' = 0)$ complex with a He atom localized in the antilinear well. It would be interesting to perform theoretical simulations of the formation and subsequent cooling of the $He_m\cdots{}^{79}Br_2(X, v'' = 0)$ and $He_m\cdots I^{35}Cl(X, v'' = 0)$ complexes to determine if these processes do not efficiently stabilize particular conformers using the expansion conditions that we have implemented. Experimental and theoretical efforts focusing on the stabilization of weakly bound complexes provide an additional venue for characterizing the multidimensional PESs, and the information gleaned from these studies complements quite well the study of dissociation dynamics in these systems.

D. Comparison with Theoretical Results. The structure, energetics, and dynamics of $He_2\cdots Br_2(X, v'' = 0)$ and $He_2\cdots ICl(X, v'' = 0)$ complexes have been investigated using ab initio electronic structure and quantum-mechanical calculations.[48−51] The potential energies and binding energies associated with these complexes are summarized in Table 1 for clarity. The calculations of the $2He + Br_2(X, v'' = 0)$ intermolecular PES indicate that there are three distinct minima.[48] Calculations at the CCSD(T) level of theory indicate the global minimum has an energy of −89.18 cm^{-1}. This minimum has a linear geometry with one He atom localized at each end of the Br_2 molecule, which would be associated with the (0, 2)$He_2\cdots Br_2(X, v'' = 0)$ conformer. The other minima are associated with the (1, 1)$He_2\cdots Br_2(X, v'' = 0)$ and (2, 0)$He_2\cdots Br_2(X, v'' = 0)$ conformers with potential energies of −80.78 and −74.02 cm^{-1}, respectively. The He···He interactions are strong enough to result in a tetrahedral geometry for the (2, 0)$He_2\cdots Br_2(X, v'' = 0)$ conformer.

TABLE 1: Calculated and Experimental Well Depths, D_e, and Binding Energies, D_0, of (#T, #L)$He_m\cdots I^{35}Cl(X, v'' = 0)$ and (#T, #L)$He_m\cdots{}^{79}Br_2(X, v'' = 0)$ Complexes[a]

		$He_m\cdots I^{35}Cl$		$He_m\cdots{}^{79}Br_2$	
		calcd	exptl	calcd	exptl
(1, 0)	D_0	15.15[b]	16.6(3)[c]	15.81[d]	16.6(8)[d]
	D_e	38.96[e]		40.64[d]	
(0, 1)	D_0	18.29[b]	22.0(2)[f]	16.46[d]	17.0(8)[d]
	D_e	58.62[e]		49.45[d]	
(2, 0)	D_0	30.46[g]	33.2(4)	30.93[h]	33.2(1.1)
	D_e	88.32[g]		74.02[h]	
(1, 1)	D_0	33.51[g]	38.6(4)	31.44[h]	33.6(1.1)
	D_e	99.12[g]		80.78[h]	
(0, 2)	D_0	31.60[g]		32.34[h]	
	D_e	97.42[g]		89.18[h]	

[a] The notation (#T, #L)$He_m\cdots XY$ is described in the text and is used to identify the number of He atoms localized in the T-shaped, #T, and linear, #L, wells about the dihalogen molecule. Energies are in cm^{-1} and represent the energies below the mHe + $I^{35}Cl(X, v'' = 0)$ and mHe + $^{79}Br_2(X, v'' = 0)$ asymptotes. [b] Reference 2. [c] Reference 39. [d] Reference 3. [e] Reference 9. [f] Reference 1. [g] Reference 49. [h] Reference 48.

Variational calculations using a sum of $He\cdots Br_2$ three-body interactions have been performed to find the bound levels of the $He_2\cdots{}^{79}Br_2(X, v'' = 0)$ ground-state complex.[48] The probability amplitudes of the three lowest energy levels, labeled as $n'' = 0-2$, are each localized in the different minima of the PES, indicating that these levels can be referred to as different conformers of the $He_2\cdots Br_2(X, v'' = 0)$ complex. The ordering of the energy levels follows the energies of the potential minima, with the $n'' = 0$ level having a linear (0, 2)$He_2\cdots Br_2$ geometry, the $n'' = 1$ level having a (1, 1)$He_2\cdots Br_2$ geometry, and the $n'' = 2$ level having the tetrahedral (2, 0)$He_2\cdots Br_2$ geometry. The binding energies of the $n'' = 0$, $n'' = 1$, and $n'' = 2$ levels have been calculated to be 32.24, 31.44, and 30.93 cm^{-1}, respectively. These values are only slightly larger than those obtained by assuming weak He···He interactions and summing the calculated energies of the appropriate n'' levels for the $He\cdots Br_2(X, v'' = 0)$ complex. The calculated binding energies of the linear (0, 1)$He\cdots Br_2$ and T-shaped (1, 0)$He\cdots Br_2$ conformers are 16.46 and 15.81 cm^{-1}, respectively.[3] Using these values, the binding energies of the linear (0, 2)$He_2\cdots Br_2$ and tetrahedral (2, 0)$He_2\cdots Br_2$ conformers are approximated as twice those of the linear (0, 1)$He\cdots Br_2$ and T-shaped (1, 0)$He\cdots Br_2$ complexes, respectively, or 32.92 and 31.62 cm^{-1}. The binding energy of the (1, 1)$He_2\cdots Br_2$ conformer could be approximated as the sum of the T-shaped and linear $He\cdots Br_2$ conformers, 32.27 cm^{-1}.

In a similar manner, we can also use the experimentally measured binding energies of the linear (0, 1)$He\cdots{}^{79}Br_2(X, v'' = 0)$ and T-shaped (1, 0)$He\cdots{}^{79}Br_2(X, v'' = 0)$ conformers to approximate the binding energies of the (1, 1)$He_2\cdots{}^{79}Br_2(X, v'' = 0)$ and (2, 0)$He_2\cdots{}^{79}Br_2(X, v'' = 0)$ conformers. The binding energy of the linear (0, 1)$He\cdots{}^{79}Br_2(X, v'' = 0)$

conformer was measured to be 17.0(8) cm^{-1}.[3] Using a simplistic thermodynamic model, we estimated the binding energy of the T-shaped (1, 0)He···$^{79}Br_2$(X, $v'' = 0$) conformer to be 16.6(8) cm^{-1}.[3] By summing these binding energies, we approximate a binding energy of 33.6(1.1) cm^{-1} for the (1, 1)He_2···$^{79}Br_2$(X, $v'' = 0$) conformer. This value is just greater than the calculated value of 31.44 cm^{-1} for the $n'' = 1$ level, and the value of 32.27 cm^{-1} approximated for this conformer. An experimental estimate of the binding energy of the (2, 0)He_2···$^{79}Br_2$(X, $v'' = 0$) conformer can be taken as twice that of the T-shaped (1, 0)He···$^{79}Br_2$(X, $v'' = 0$) conformer, or 33.2(1.1) cm^{-1}. Again, this energy is slightly larger than the calculated valued for the $n'' = 2$ level, 30.93 cm^{-1}, and that approximated for this conformer, 31.62 cm^{-1}. To date, we have not yet identified spectroscopic features associated with transitions of the linear (0, 2)He_2···$^{79}Br_2$(X, $v'' = 0$) conformer, which is predicted to be the most stable conformer.

The electric dipole of ICl and the increased reduced mass of the complex give rise to an enhanced interaction of He with ICl in the linear geometry in comparison with the He···Br_2 interactions.[49] The calculations indicate that there are five distinct minima in the 2He + ICl(X, $v'' = 0$) PES.[49] The (1, 1)He_2···ICl(X, $v'' = 0$) conformer is the most stable structure with an energy of −99.12 cm^{-1} relative to the 2He + ICl(X, $v'' = 0$) asymptote. The (0, 2)He_2···ICl(X, $v'' = 0$) conformer with one He atom at the I-atom end and the other He atom at the Cl-atom end has the next lowest energy, −97.42 cm^{-1}. The next minimum, at −88.32 cm^{-1}, has the (2, 0)He_2···ICl(X, $v'' = 0$) configuration with the two He atoms weakly bound to each other, thereby resulting in a tetrahedral geometry. The well depths of the last two minima, not included in Table 1, are −85.84 and −78.54 cm^{-1}. The minimum at −78.54 cm^{-1} has a (1, 1)He_2···ICl(X, $v'' = 0$) configuration, where one He atom is localized at the Cl-atom end and the other is in the T-shaped minimum, and the minimum at −85.84 cm^{-1} corresponds to a (0, 2)He_2···ICl(X, $v'' = 0$) configuration, where both He atoms are localized in the well at the I-atom end of the ICl molecule.

The intermolecular vibrational levels bound within the 2He + ICl(X, $v'' = 0$) ground-state PES have been calculated using the variational method.[49] The probability amplitudes of the five lowest intermolecular vibrational levels indicate that the He atoms are localized in distinct minima around the ICl molecule, and we refer to these levels as different conformers of the He_2···ICl(X, $v'' = 0$) complex. The binding energies of the (1, 1)He_2···ICl(X, $v'' = 0$), (0, 2)He_2···ICl(X, $v'' = 0$), and (2, 0)He_2···ICl(X, $v'' = 0$) conformers have been calculated to be 33.51, 31.60, and 30.46 cm^{-1}. These values are similar to those approximated by summing the calculated energies of the He···ICl(X, $v'' = 0$) conformers. The calculated binding energies of the linear (0, 1)He···ICl and T-shaped (1, 0)He···ICl conformers are 18.29 and 15.14 cm^{-1}.[2] The antilinear (0, 1)He···ICl conformer, which has the He atom localized at the Cl end of ICl, has a calculated binding energy of 11.76 cm^{-1}. Using these He···ICl energies, the binding energies of the (1, 1)He_2···ICl, the tetrahedral (2, 0)He_2···ICl, and the linear (0, 2)He_2···ICl conformers are approximated as 33.43, 30.28, and 30.05 cm^{-1}, respectively.

Using the experimentally measured binding energies of the (0, 1)He···ICl(X, $v'' = 0$) and (1, 0)He···ICl(X, $v'' = 0$) conformers, 22.0(2) and 16.6(3) cm^{-1}, respectively,[1,39] we approximate a binding energy of 38.6(4) cm^{-1} for the (1, 1)He_2···ICl(X, $v'' = 0$) conformer. The next higher calculated level, $n'' = 1$, is the linear (0, 2)He_2···ICl(X, $v'' = 0$) conformer with a binding energy of 31.60 cm^{-1}, but this level and that of the antilinear (0, 1)He···ICl(X, $v'' = 0$) conformer were not experimentally observed. We assume that we can multiply the experimental binding energy of the (1, 0)He···ICl(X, $v'' = 0$) conformer by two to account for the two He atoms within the T-shaped well, and we get an experimental energy of 33.2(4) cm^{-1} for the (2, 0)He_2···ICl(X, $v'' = 0$) conformer. This energy is slightly greater than that calculated for the $n'' = 2$ level. Nevertheless, the calculations find (1, 1)He_2···ICl(X, $v'' = 0$) to be the most stable conformer, lying 3.05 cm^{-1} lower in energy than the (2, 0)He_2···ICl(X, $v'' = 0$) conformer. Experimentally, we find the same ordering with an approximated energy difference of 5.4(6) cm^{-1} between the two conformers.

IV. Conclusions

We have spectroscopically identified multiple conformers of the He_2···$^{79}Br_2$(X, $v'' = 0$), He_3···$^{79}Br_2$(X, $v'' = 0$), He_2···$I^{35}Cl$(X, $v'' = 0$), and He_3···$I^{35}Cl$(X, $v'' = 0$) complexes. Specifically, we have recorded action spectra in the B−X, v'−0 regions with the probe laser fixed on transitions probing different Br_2(B, v) and ICl(B, v) dissociation channels. The transition energies of the spectral features associated with the different conformers follow a band-shift rule, $\nu = \nu_0 + \{(\#T)\Delta\nu_T + (\#L)\Delta\nu_L\}$, where ν_0 is the energy of the monomer band origin, $\Delta\nu_T$ is the shift of the T-shaped (1, 0)He···$^{79}Br_2$ or (1, 0)He···$I^{35}Cl$ feature from ν_0, and $\Delta\nu_L$ is the shift of the linear (0, 1)He···$^{79}Br_2$ or (0, 1)He···$I^{35}Cl$ feature from ν_0. For the (#T, #L)He_m···$^{79}Br_2$ or (#T, #L)He_m···$I^{35}Cl$ higher-order complexes, the features associated with conformers that have #T and #L He atoms localized in the T-shaped and linear wells of the intermolecular PES can be accurately predicted.

We have identified two conformers for the He_2···$^{79}Br_2$(X, $v'' = 0$) and He_2···$I^{35}Cl$(X, $v'' = 0$) complexes, one with (2, 0) and the other with (1, 1) configurations. For the He_3···$I^{35}Cl$(X, $v'' = 0$) complex, we have identified two ground-state conformers, the (3, 0) and (2, 1) conformers. A third conformer was observed for the He_3···$^{79}Br_2$(X, $v'' = 0$) complex, the (1, 2) conformer. By varying the backing pressure of the carrier gas and the downstream distance at which the spectra are recorded, we have shown that the (1, 1) conformer is energetically more stable than the (2, 0) conformer for both the He_2···$^{79}Br_2$(X, $v'' = 0$) and He_2···$I^{35}Cl$(X, $v'' = 0$) complexes. The energetic ordering of the conformers is in agreement with theoretical calculations of these levels.

Acknowledgment. R.A.L. is indebted to the David and Lucile Packard Foundation for a Fellowship in Science and Engineering and to the National Science Foundation for a CAREER Award, CHE-0346745.

References and Notes

(1) Boucher, D. S.; Darr, J. P.; Bradke, M. D.; Loomis, R. A.; McCoy, A. B. *Phys. Chem. Chem. Phys.* **2004**, *6*, 5275.
(2) McCoy, A. B.; Darr, J. P.; Boucher, D. S.; Winter, P. R.; Bradke, M. D.; Loomis, R. A. *J. Chem. Phys.* **2004**, *120*, 2677.
(3) Boucher, D. S.; Strasfeld, D. B.; Loomis, R. A.; Herbert, J. M.; Ray, S. E.; McCoy, A. B. *J. Chem. Phys.* **2005**, *123*, 104312.
(4) Darr, J. P.; Glennon, J. J.; Loomis, R. A. *J. Chem. Phys.* **2005**, *122*, 131101.
(5) Ray, S. E.; McCoy, A. B.; Glennon, J. J.; Darr, J. P.; Fesser, E. J.; Lancaster, J. R.; Loomis, R. A. *J. Chem. Phys.* **2006**, *125*, 164314.
(6) Boucher, D. S.; Loomis, R. A. *Adv. Chem. Phys.* **2008**, *138*, 375.
(7) Buchachenko, A. A.; Prosmiti, R.; Cunha, C.; Delgado-Barrio, G.; Villarreal, P. *J. Chem. Phys.* **2002**, *117*, 6117.
(8) Cunha, C.; Prosmiti, R.; Villarreal, P.; Delgado-Barrio, G. *Mol. Phys.* **2002**, *100*, 3231.
(9) Prosmiti, R.; Cunha, C.; Villarreal, P.; Delgado-Barrio, G. *J. Chem. Phys.* **2002**, *117*, 7017.

(10) Prosmiti, R.; Cunha, C.; Villarreal, P.; Delgado-Barrio, G. *J. Chem. Phys.* **2002**, *116*, 9249.
(11) Prosmiti, R.; Valdés, A.; Villarreal, P.; Delgado-Barrio, G. *J. Phys. Chem. A* **2004**, *108*, 6065.
(12) Valdés, A.; Prosmiti, R.; Villarreal, P.; Delgado-Barrio, G. *Mol. Phys.* **2004**, *102*, 2277.
(13) Delgado-Barrio, G.; Prosmiti, R.; Valdés, Á.; Villarreal, P. *Phys. Scr.* **2006**, *73*, C57.
(14) Sharfin, W.; Johnson, K. E.; Wharton, L.; Levy, D. H. *J. Chem. Phys.* **1979**, *71*, 1292.
(15) Kenny, J. E.; Johnson, K. E.; Sharfin, W.; Levy, D. H. *J. Chem. Phys.* **1980**, *72*, 1109.
(16) Johnson, K. E.; Sharfin, W.; Levy, D. H. *J. Chem. Phys.* **1981**, *74*, 163.
(17) Swartz, B. A.; Brinza, D. E.; Western, C. M.; Janda, K. C. *J. Phys. Chem.* **1984**, *88*, 6272.
(18) Hair, S. R.; Cline, J. I.; Bieler, C. R.; Janda, K. C. *J. Chem. Phys.* **1989**, *90*, 2935.
(19) Drobits, J. C.; Lester, M. I. *J. Chem. Phys.* **1987**, *86*, 1662.
(20) Sands, W. D.; Bieler, C. R.; Janda, K. C. *J. Chem. Phys.* **1991**, *95*, 729.
(21) Bacic, Z.; Kennedy-Mandziuk, M.; Moskowitz, J. W. *J. Chem. Phys.* **1992**, *97*, 6472.
(22) Hernández, M. I.; Halberstadt, N. *J. Chem. Phys.* **1994**, *100*, 7828.
(23) Villarreal, P.; Roncero, O.; Delgado-Barrio, G. *J. Chem. Phys.* **1994**, *101*, 2217.
(24) Garcia-Rizo, C.; Hernández, M. I.; Garcia-Vela, A.; Villarreal, P.; Delgado-Barrio, G. *J. Mol. Struct.* **1999**, *493*, 125.
(25) Hernández, M. I.; Halberstadt, N.; Sands, W. D.; Janda, K. C. *J. Chem. Phys.* **2000**, *113*, 7252.
(26) Rohrbacher, A.; Halberstadt, N.; Janda, K. C. *Annu. Rev. Phys. Chem.* **2000**, *51*, 405.
(27) Blazy, J. A.; DeKoven, B. M.; Russell, T. D.; Levy, D. H. *J. Chem. Phys.* **1980**, *72*, 2439.
(28) Burroughs, A.; Heaven, M. C. *J. Chem. Phys.* **2001**, *114*, 7027.
(29) Drobits, J. C.; Skene, J. M.; Lester, M. I. *J. Chem. Phys.* **1986**, *84*, 2896.
(30) Skene, J. M.; Drobits, J. C.; Lester, M. I. *J. Chem. Phys.* **1986**, *85*, 2329.
(31) Boucher, D. S.; Bradke, M. D.; Darr, J. P.; Loomis, R. A. *J. Phys. Chem. A* **2003**, *107*, 6901.
(32) Bradke, M. D.; Loomis, R. A. *J. Chem. Phys.* **2003**, *118*, 7233.
(33) Strasfeld, D. B.; Darr, J. P.; Loomis, R. A. *Chem. Phys. Lett.* **2004**, *397*, 116.
(34) Chandra, P. P.; Stephenson, T. A. *J. Chem. Phys.* **2004**, *121*, 2985.
(35) Hutchison, J. M.; Carlisle, B. R.; Stephenson, T. A. *J. Chem. Phys.* **2006**, *125*, 194313.
(36) Stephenson, T. A.; Hong, Y.; Lester, M. I. *J. Chem. Phys.* **1991**, *94*, 4171.
(37) Stephenson, T. A.; Hong, Y.; Lester, M. I. *Chem. Phys. Lett.* **1989**, *159*, 549.
(38) Tscherbul, T. V.; Buchachenko, A. A.; Akopyan, M. E.; Poretsky, S. A.; Pravilov, A. M.; Stephenson, T. A. *Phys. Chem. Chem. Phys.* **2004**, *6*, 3201.
(39) Darr, J. P.; Loomis, R. A. *J. Chem. Phys.* **2008**, *129*, 144306.
(40) Jahn, D. G.; Barney, W. S.; Cabalo, J.; Clement, S. G.; Rohrbacher, A.; Slotterback, T. J.; Williams, J.; Janda, K. C. *J. Chem. Phys.* **1996**, *104*, 3501.
(41) van de Burgt, L. J.; Nicolai, J.-P.; Heaven, M. C. *J. Chem. Phys.* **1984**, *81*, 5514.
(42) Valdés, A.; Prosmiti, R.; Villarreal, P.; Delgado-Barrio, G. *J. Chem. Phys.* **2005**, *122*, 044305.
(43) Darr, J. P.; Loomis, R. A.; McCoy, A. B. *J. Chem. Phys.* **2005**, *122*, 044318.
(44) Cabrera, J. A.; Bieler, C. R.; Olbricht, B. C.; van der Veer, W. E.; Janda, K. C. *J. Chem. Phys.* **2005**, *123*, 054311.
(45) García-Vela, A.; Janda, K. C. *J. Chem. Phys.* **2006**, *124*, 034305.
(46) Smalley, R. E.; Levy, D. H.; Wharton, L. *J. Chem. Phys.* **1976**, *64*, 3266.
(47) Bastida, A.; Zúñiga, J.; Requena, A.; Miguel, B.; Beswick, J. A.; Vigué, J.; Halberstadt, N. *J. Chem. Phys.* **2002**, *116*, 1944.
(48) Valdés, Á.; Prosmiti, R.; Villarreal, P.; Delgado-Barrio, G. *J. Chem. Phys.* **2005**, *122*, 044305.
(49) Valdés, Á.; Prosmiti, R.; Villarreal, P.; Delgado-Barrio, G. *J. Chem. Phys.* **2006**, *125*, 014313.
(50) de Lara-Castells, M. P.; Prosmiti, R.; Delgado-Barrio, G.; López-Durán, D.; Villarreal, P. *Phys. Rev. A* **2006**, *74*, 053201.
(51) Diez-Pardos, C.; Valdés, Á.; Prosmiti, R.; Villarreal, P.; Delgado-Barrio, G. *Theor. Chem. Acc.* **2007**, *118*, 511.

JP808368J